Sol-gel Derived Poly(vinyl alcohol)/Maleic Acid/Silica Hybrid Membrane for Desalination by Pervaporation

Zongli Xie[a,b], Manh Hoang[a], Tuan Duong[a], Derrick Ng[a], Buu Dao[a], Stephen Gray[b]

a CSIRO Materials Science and Engineering, Private Bag 33, Clayton South, Vic.3169, Australia (Email: zongli.xie@csiro.au; manh.hoang@csiro.au; tuan.duong@csiro.au; derrick.ng@csiro.au, buu.dao@csiro.au)
b Institute for Sustainability and Innovation, Victoria University, PO Box 14428, Melbourne, Vic. 8001, Australia (E-mail: stephen.gray@vu.edu.au)

Abstract
Highly dispersed homogeneous hybrid polymer-inorganic membranes based on poly(vinyl alcohol) (PVA), maleic acid (MA) and inorganic silica were synthesized via a sol-gel method. Tetraethoxy-silane (TEOS) was used as the silica precursor with MA as an additional crosslinking agent. A range of techniques such as FTIR, SEM, TGA, XRD and DSC were used to characterise the nanostructure and properties of hybrid membranes. Results revealed silica nanoparticles (<10 nm) were well dispersed in the polymer matrix with chemical bonding between the organic and inorganic phases. Thermal properties of the hybrid membranes were significantly enhanced when compared with pure PVA membranes, and swelling of PVA based hybrid membranes was greatly suppressed.

The chemically crosslinked PVA with maleic acid and silica resulted in the formation of new hybrid membranes with improved pervaporation properties for desalination application. The pervaporation separation performance of aqueous salt solution was found to be directly related to the diffusion coefficient of water through hybrid PVA/MA/silica membranes. Introduction of MA and silica at given amounts into the polymer chain increased the amorphous region of the membrane and favoured the diffusion of water molecules through the membrane. A water flux of 6.93 kg/m^2·hr with salt rejection of >99.5% was achieved at a 6 Torr vacuum and 22°C.

Keywords
Poly(vinyl alcohol); hybrid organic-inorganic membrane; sol-gel; silica; maleic acid; desalination

1. INTRODUCTION

In recent years, membrane desalination using reverse osmosis (RO) has been the leading candidate technology for supplying fresh water. Generally, the main limitations of RO technology are the overall high energy cost and the sensitivity of RO membrane elements to fouling. Therefore, there is a strong motivation for improving the established membrane process and/or developing alternative membrane technologies. In the later context, pervaporation is a potential low energy membrane technology as it has the advantage that the energy need is essentially independent of the concentration of the salt feed water. The pervaporation process combines the evaporation of volatile components of a mixture with their permeation through a nonporous polymeric membrane under reduced pressure conditions [1, 2]. During pervaporation, the feed mixture is in direct contact with one side of the hydrophilic membrane and the permeate is removed in a vapour state from the permeate side. Transport through the membrane is driven by the vapour pressure difference between the feed solution and the permeate vapour. The vapour pressure difference is generally created by applying a vacuum or by sweeping an inert gas on the permeate side of the membrane.

Pervaporation has been extensively used for separation or concentration of mixtures of aqueous-organic or organic liquids. However, there is little published information on application of this technology for water desalination. In desalination applications, pervaporation has the advantage of near 100% of salt rejection. The pervaporation of an aqueous salt solution can be regarded as

1

separation of a pseudo-liquid mixture containing free water molecules and bulkier hydrated ions formed in solution upon dissociation of the salt in water [1]. Previous studies have demonstrated the possibility of applying pervaporation to produce distilled water from aqueous salt solutions [1, 3]. However, the water flux reported so far is generally quite low, at <6 L/m^2·hr [4, 5]. One of the main limitations for desalination using pervaporation is the lack of the high performance membranes with both high permeate flux and good salt rejection.

Polymer-inorganic nanocomposite materials, in which polymers serve as hosts for inorganic nano-particles, are promising materials for many applications due to their extraordinary properties. The combination of these two different building blocks at a molecular level could provide novel properties that are not obtained from conventional organic or inorganic materials [6-9]. The sol-gel method is a common process to synthesise polymer-inorganic nanocomposites. It consists of an initial hydrolysis reaction, a subsequent condensation reaction followed by removal of the solvents, resulting in formation of metal oxides.

Poly(vinyl alcohol) (PVA), a water soluble hydrophilic polymer, has been studied intensively for membrane applications because of its good chemical stability, film-forming ability and high hydrophilicity. High hydrophilicity is critical for desalination membranes to minimise membrane fouling by natural organic matter [10]. However, PVA has poor stability in water. Therefore, it must be insolubilised by modification reactions such as grafting [11] or crosslinking [12, 13] to form a stable membrane with good mechanical properties and selective permeability to water. Among various insolubilisation techniques, hybridisation between PVA and inorganic particles has received significant interest as it not only restricts the swelling of PVA but also provides the inherent advantages of the organic and inorganic compounds [14]. Previous studies have shown that introducing an inorganic component derived from Si-containing precursors into PVA can form a homogeneous nanocomposite membrane with enhanced physicochemical stability and separation performance in pervaporation separation of benzene/cyclohexane mixtures [9, 15] and aqueous ethanol solution [15]. However, there is little published result on application of this type of membranes for pervaporation desalination.

This paper reports the development of a new type of hybrid polymer-inorganic membrane based on PVA/MA/silica for desalination by pervaporation. The hybrid membrane was synthesised via a sol-gel route by using tetraethoxy-silane (TEOS) as the silica precursor with maleic acid (MA) as an additional crosslinking agent. The resulting hybrid membranes with varying silica and MA contents were characterised with a range of techniques including FTIR, SEM, WAXD, TGA, DSC and contact angle. The pervaporation separation of aqueous salt solution of hybrid PVA/MA/silica membranes was examined in relation to the diffusion coefficient of water.

2. EXPERIMENTAL

2.1 Hybrid membrane synthesis

PVA (98+% hydrolysed, molecular weight of 130,000 g/mol), TEOS (98%), MA and sodium chloride (NaCl) were obtained from Sigma-Aldrich and used without further purification. Milli-Q deionised water (18.1 MΩ·cm@25°C) was used to prepare PVA solution and aqueous salt solutions. The PVA/MA/silica hybrid membranes were synthesised via an aqueous route. PVA polymer powder (0.75 g) was fully dissolved in 100 mL of Milli-Q deionised water in a silicone oil bath at 90°C. The obtained 0.75 wt% PVA solution was allowed to cool to room temperature (22°C) and the pH adjusted to 1.7±0.1 with ~0.5 mL concentrated HCl. Then 0.15 g of MA (the weight content of MA with respect to PVA = 20 wt%) was added to the PVA solution and stirred

till fully dissolved. Under steady stirring, a predetermined TEOS and ethanol mixture (mass ratio of TEOS: ethanol = 1:9) was added drop wise to the above solution. The amount of TEOS was added in the SiO_2 weight percentages of 10 and 25 wt% with respect to the amount of PVA in the solution, i.e. the weight content of SiO_2 with respect to PVA = 10-25 wt%. The reaction was held at room temperature for 2 hr. The resulting homogeneous mixture was filtered and casted on Perspex Petri dishes to the desired thickness and dried in air. Finally, the obtained film sample was dried at 50°C overnight and heated to 140°C for 2 hr in a fan forced oven. Pure PVA membrane samples were also prepared as a reference for comparison. The thickness of membranes was measured at different spots using a Fowler electronic digital micrometer (accuracy ±1 μm) and the average thickness of 6 measurements was reported and used in the study.

2.2   Material characterisation

FTIR: Fourier transform infrared spectroscopy (FTIR) was performed on a Perkin-Elmer Spectrum 2000 FTIR instrument to assess the functional structure of hybrid membrane samples. FTIR spectra of thin films were obtained with an 8 cm^{-1} resolution, from 600 to 4000 cm^{-1} wavelength.

DSC: Differential scanning calorimetry (DSC) was conducted using a Perkin-Elmer Pyris-1 differential scanning calorimeter to assess the glass transition temperature (T_g) of PVA and its hybrid membrane samples. The analysis was conducted under nitrogen with samples of approximately 5-10 mg at a scan rate of 10°C min^{-1} from 10 to 250°C. T_g was calculated by the half C_p extrapolated method using the Pyris-1 DSC software.

TGA: Thermal stabilities of PVA and hybrid membranes were assessed using a Perkin-Elmer Pyris 1 thermogravimetry analysis (TGA) instrument. Experiments were conducted on 3-5 mg thin film samples heated in flowing nitrogen at a heating rate of 10°C min^{-1} from 30 to 800°C.

Morphology: The morphology of the hybrid membrane samples were imaged using a TECNAI F30 Transmission electron microscope (TEM) with an accelerating voltage of 200 kV. TEM samples were prepared by a focused ion beam (FIB) technique. Energy dispersive X-ray spectrometry (EDS) was performed by an EDAX detector on a Philips XL30 scanning electronic microscope (SEM)with a voltage of 15 kV and a working distance of 15 mm. Membrane samples were coated by sputtering with gold for FIB and with carbon for EDS.

WAXD: The crystalline diffraction of PVA and hybrid membranes were studied at room temperature using a Bruker D8 advanced wide-angle X-ray diffractometer (WAXD) with Cu-Kα radiation (40kV, 40mA) monochromatised with a graphite sample monochromator. Dried membrane samples were mounted on zero background plates and scanned over a 2θ range of 5 to 61° with a step size of 0.02° and a count time of 4 seconds per step.

Swelling properties: The dried membrane samples were immersed in deionised water at room temperature for 48 h to reach the absorption equilibrium. Wet membranes were then blot dried with cleansing tissues and quickly weighed within 10 sec (wet membrane) following which the membrane was dried in a vacuum oven at 50°C for overnight and then weighed (dried membrane). Two tests were conducted on each sample. The swelling degree (*S*) of membrane was calculated according to:

$$S = \frac{W_s - W_d}{W_d} \times 100\% \qquad (1)$$

Where W_s and W_d are the weight of wet and dry membrane, respectively.

Contact angle: The hydrophilic properties of membrane samples were assessed by a KSV contact angle meter (CAM200) equipped with an image capturing system. Static contact angles were measured by the sessile drop method. A 6 µL water drop was formed on the levelled surface of the membrane for contact angle measurements.
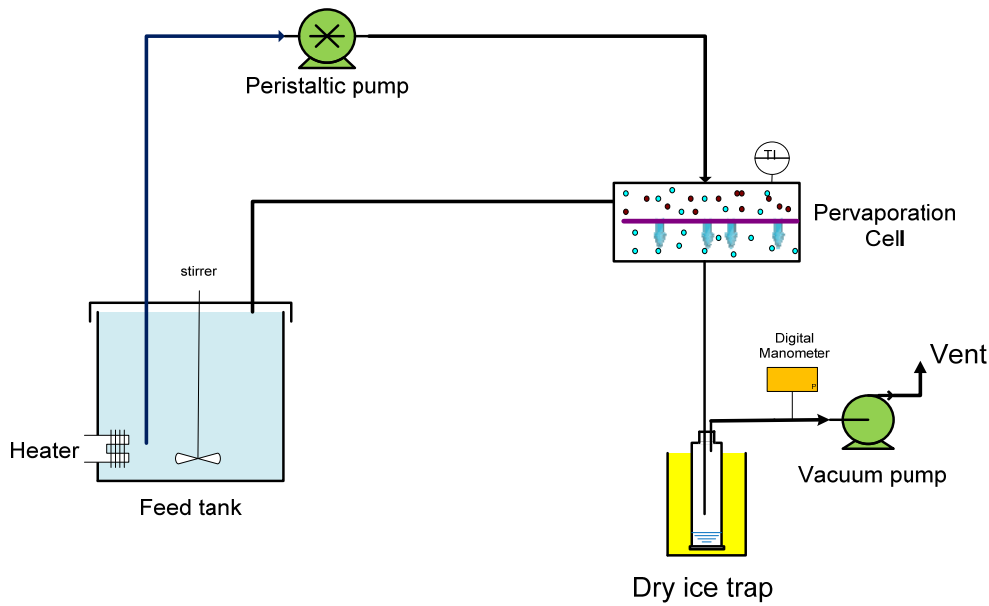
2.3 Pervaporation testing

Figure 1. Schematic drawing of the pervaporation unit.

The pervaporation experiments were carried out on a laboratory scale pervaporation unit as shown in Figure 1. The membrane was placed in the middle of a pervaporation cell and the effective surface area of the membrane was 12.6 cm². An aqueous solution containing 2000 ppm NaCl was used as the feed solution. During the experiment, the feed solution was preheated in a water bath to the required temperature and pumped to the pervaporation cell using a Masterflex® peristaltic pump. The pressure on the permeate side of the membrane cell was maintained at 6 Torr with a vacuum pump. The permeate was collected in a dry-ice cold trap. A K-type thermocouple installed in the feed chamber was used to measure the operating temperature of feed solution and the feed temperature was varied from 22 to 65°C in the study.

The pervaporation desalination performance of hybrid membranes were characterised by water flux and salt rejection. The water flux (J) was determined from the mass (M) of permeate collected in the cold trap, the effective membrane area (A) and the experimental time (t).

$$J = \frac{M}{A * t} \qquad (2)$$

The salt concentration of the feed (C_f) and permeate (C_p) were derived from measured conductivity with an Oakton[®] Con 110 conductivity meter. The conductivity meter was calibrated using a series of prepared standard NaCl solutions with known concentration in the range of 0-7700 ppm. A calibration curve and equation between NaCl concentration and conductivity were then constructed and used to calculate NaCl concentration. The salt rejection (R) was determined by the following equation:

$$R = \frac{C_f - C_p}{C_f} \times 100\% \qquad\qquad (3)$$

Each experiment was run for 3 hours. At the end of each experiment, the downstream (permeate side) of the membrane cell was flushed with a known amount of de-ionised water and the conductivity of this stream was measured to check the salt leaking or crystallisation. In the study, hybrid membranes remained clean and there was no evidence of salt precipitation or crystallisation on the permeate side of the membrane. The results during pervaporation testing were reproducible, with the variation generally within ±0.2 kg/m^2·hr for water flux and ±1.0% for salt rejection.

Diffusion coefficient is an important factor to estimate the diffusion of the penetrants through membranes and permeation flux. Based on Fick's law, the permeation flux of component i can be expressed as [9, 16, 17]

$$J_i = -D_i \frac{dC_i}{dx} \qquad\qquad (4)$$

Where J_i, D_i and C_i are the permeation flux (kg/m^2·hr), the diffusion coefficient (m^2/s) and the concentration (kg/m^3) of component i in the membranes, respectively; x is the diffusion length (m). For simplicity, the apparent diffusion coefficient can be calculated by the equation [17]:

$$D_i = \frac{J_i \delta}{C_{i,f}} \qquad\qquad (5)$$

Where δ is the membrane thickness, and $C_{i,f}$ is the concentration of component i in the feed.

3. RESULTS & DISCUSSION

3.1 FTIR analysis

Figure 2 shows the ATR-FTIR spectra of PVA/silica and PVA/MA/silica membrane with a pure PVA sample as a reference. FTIR spectra confirmed the formation of PVA/MA and PVA/MA/silica hybrid with network crosslinking. The pure PVA sample (Figure 1-a) shows the typical C-H broad alkyl stretching band (2800-3000 cm^{-1}) and the hydrogen bonded hydroxyl band (3200-3570 cm^{-1}) [18]. The peak at 1000-1100 cm^{-1} was assigned to the C-O stretching vibration of the secondary alcohol (-CH-OH) of PVA. For the hybrid PVA/silica membrane (Figure 1-b) and PVA/MA/silica membrane (Figure 1-c), it was noticed there was an increase in the peak intensity at this range. For the hybrid PVA/MA/silica membrane (Figure 1-c), there was also a new peak observed at 1726 cm^{-1} assigned to the ester group (-CO-O-) [19].

In preparing the hybrid PVA/silica and PVA/MA/silica membranes, TEOS was initially hydrolysed in the presence of acid catalyst to form silanol groups which were subsequently condensed to form

silicon oxide network. Under acid conditions, the hydrolysis reaction is more rapid than condensation reactions and linear or random branches of silica network tend to be formed [20]. The resulting silanol groups formed siloxane bonds from subsequent condensation reactions during membrane drying. These reactions led to cohesive bonds between siloxane in the membrane which were dispersed in the polymer membrane [14, 15]. In fabricating the hybrid PVA/MA/silica membranes, the hydroxyl groups in the repeating units of PVA and the carboxylic groups in MA were expected to produce strong secondary interactions with these silanol groups to form hydrogen and covalent bonds. Therefore, the increase in peak intensity at 1000-1100 cm^{-1} could be explained by the formation of Si-O-Si bonds (1080 cm^{-1}) resulting from the condensation reaction between hydrolysed silanol Si-OH groups, and also covalent Si-O-C bonds resulting from the crosslinking reaction between PVA and TEOS [14]. A new peak at 950 cm^{-1} may be attributed to Si-OH bonds resulting from the hydrolysis reaction of TEOS and the hydrogen bonds between the organic groups and the silica. Obviously, introduction of Si-OH and Si-O-Si through hydrolysis and condensation reactions of TEOS has modified the PVA structure.

In addition, PVA and MA go through esterification reactions via grafting or crosslinking under heat treatment to form the ester group. This would explain the new peak at 1726 cm^{-1} for the hybrid PVA/MA/silica membrane (Figure 1-c). In the hybrid PVA/MA/silica membrane, MA is also believed to act as an organic-inorganic coupling agent. This idea is supported by comparing the optical properties of hybrid PVA/MA/silica and PVA/silica membranes. The sample with MA (PVA/MA/silica) was clear and transparent. On the other hand, the film sample in the absence of MA (PVA/silica) was brown in colour and not transparent, as shown in Figure 3.
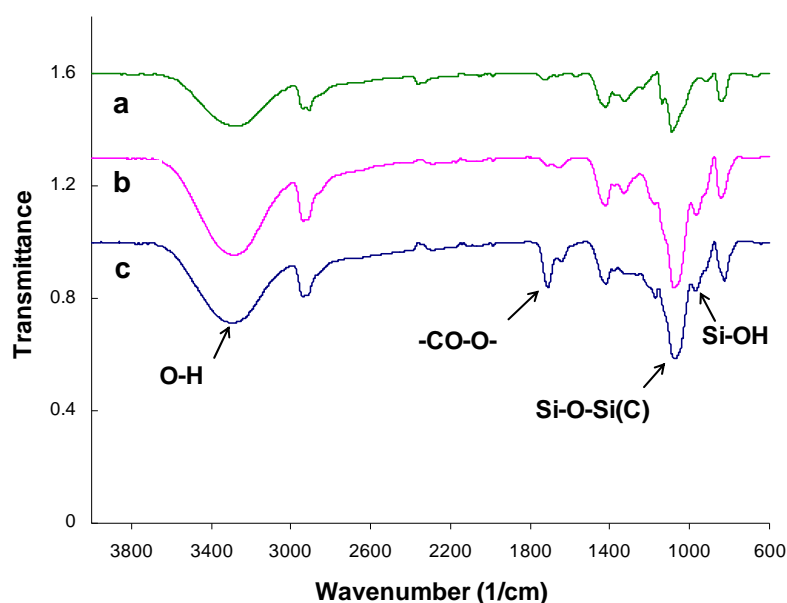

Figure 2. FTIR spectra of pure PVA and hybrid membranes (a: PVA, b: PVA/silica, 25% SiO$_2$, c: PVA/MA/silica, 20%MA and 10% SiO$_2$).
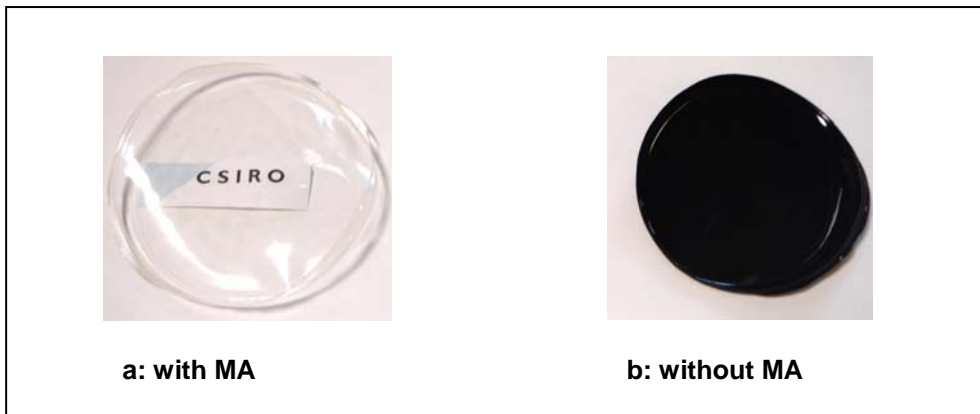
a: with MA	**b: without MA**

Figure 3. Optical images of hybrid membranes with and without MA (a: PVA/silica, 25% SiO$_2$; b: PVA/MA/silica, 20%MA and 25% SiO$_2$).

3.2 Morphology

In the hybrid polymer-inorganic membrane, the inorganic phase is dispersed in the polymer phase. It is believed that the inorganic phase, resulting from the hydrolysis and condensation of TEOS in casting solution, changes the microstructure or nanostructure of the hybrid membranes and consequently leads to the improved physical properties and performance. The uniform dispersion of silica nanoparticles and avoidance of aggregation in the polymer matrix is, therefore, critical for the performance of hybrid membranes. The phase morphology of the hybrid PVA/MA/silica membrane was studied by TEM. The typical TEM image and EDS spectra of the hybrid membrane are shown in Figure 4. The EDS spectra confirmed the formation of silica particles through sol-gel reaction of TEOS. No particles or agglomeration greater than 10 nm was observed in TEM image, indicating that the silica nanoparticles were well dispersed in the polymer matrix.

Figure 4. ... containing 20wt% MA and 10wt% SiO$_2$ wi...
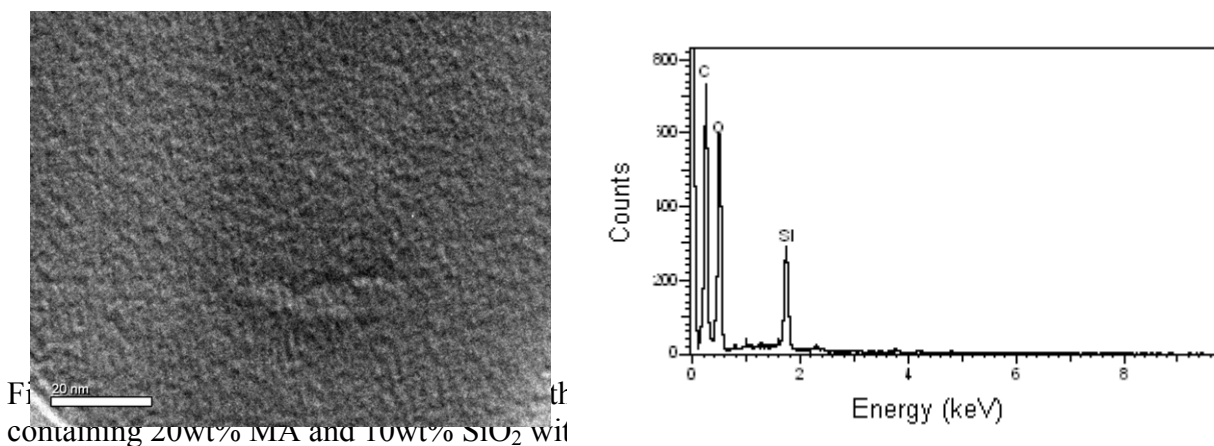
The crystallinity of PVA and its hybrid membranes was studied by WAXD analysis and the results are shown in Figure 5. For the PVA film sample, it showed a typical spectra of semi-crystalline materials and a characteristic peak of PVA appeared at approximately $2\theta = 20°$. This is in agreement with the results obtained by Kulkarni et al. [2] and Uragami [15] working with pure PVA films. With the addition of MA and silica, diffraction patterns of the hybrid membrane samples showed that the intensity of the typical peak of PVA (at 20°) became smaller (PVA/MA, PVA/silica) and the peak shape became broader (PVA/silica and PVA/MA/silica). This indicates a decrease of the crystallinity of hybrid materials and an increase of amorphous character due to the crosslinking among PVA, MA and silica. It was also noted there was a slight shift in the peak

7

position of hybrid PVA/silica and PVA/MA/silica sample. As explained by Kulkarni et al. [2] and Burshe et al.[21], this implies silanol groups of TEOS crosslink with the reactive –OH groups of PVA in a crystalline domain, leading to a more compact structure in the amorphous region due to the expansion of the crystal lattice. This is supported by the higher d-spacing value of the crystalline peak of the hybrid membrane which increased from 4.462 (PVA membrane) to 4.560 (PVA/MA/silica membrane).
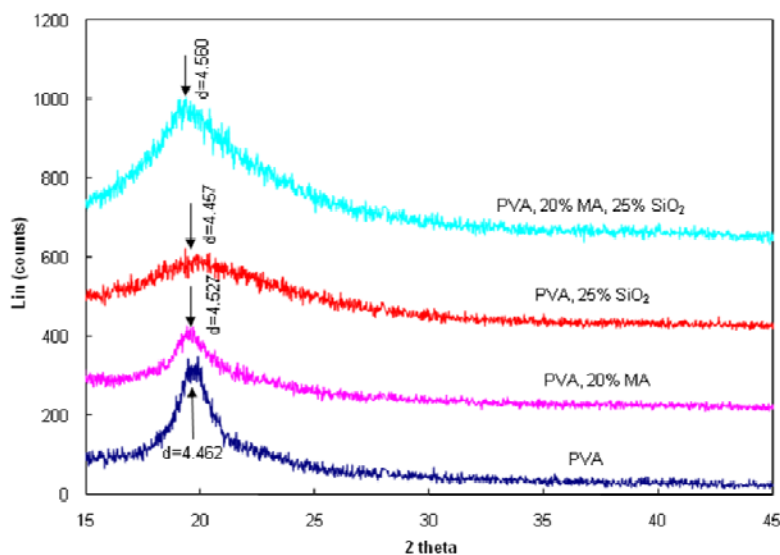

Figure 5. WAXD spectra of PVA and its hybrid membranes.

3.3 Thermal properties of hybrid membranes

Thermal gravimetric analysis (TGA) was carried out for PVA, PVA/MA, PVA/MA/silica membrane samples in the temperature range of 30-800°C under nitrogen at a heating rate of 10°C min^{-1}, with the results shown in Figure 6. Thermal stability increased for hybrid membranes. For PVA/MA membranes (Figure 6-b), both the decomposition temperature and the residual weight increased when compared with pure PVA membrane (Figure 6-a). With the addition of silica (Figure 6-c and d), the residual weight of the PVA/MA/silica membrane increased further and the degradation temperature became unclear, especially at the high silica content. When the silica content was increased from 10 wt% (sample c) to 25wt% (sample d), the residual weight increased by about the same percentage, from 21.6 wt% to 36.7 wt%.
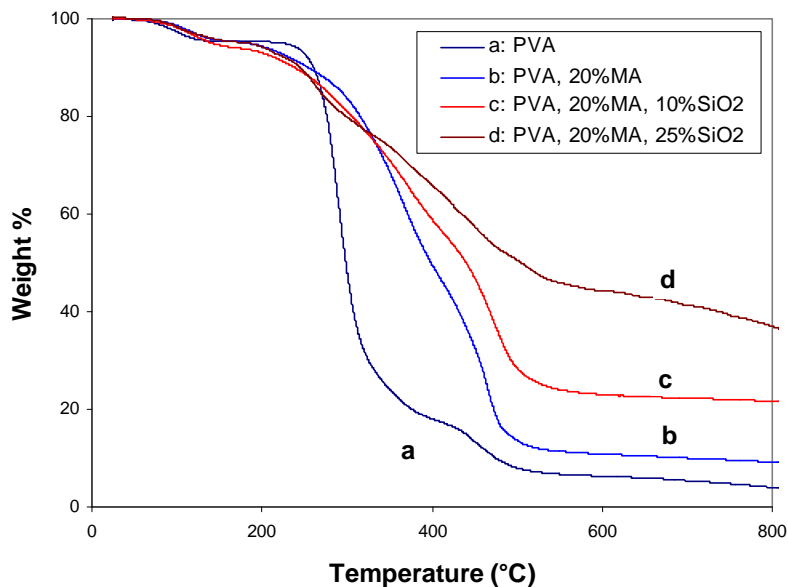
8

Figure 6. TGA curves of PVA and its hybrid membranes.

Thermal properties of these membranes were also studied by differential scanning calorimetry (DSC) performed at a heating rate of 10°C min^{-1}. Figure 7 shows the DSC thermograms of PVA and its hybrid membranes. PVA is a semi-crystalline polymer exhibiting both a glass transition temperature (T_g) and a melting isotherm (T_m), as evidenced in the DSC thermogram (Figure 7-a). The pure PVA membrane exhibited a T_g of 84°C and a T_m of 220°C. The pure PVA has the lowest T_g. For the PVA/MA membrane (Figure 7-b), the T_g increased to 94°C. The increase in T_g is consistent with an esterification reaction between MA and PVA. With the introduction of silica into the membrane (Figure 7-c), the T_g of hybrid PVA/MA/silica increased to 103°C. As the silica content increased, the T_g increased further, indicating the polymer chains were becoming more rigid with the introduction of inorganic silica.
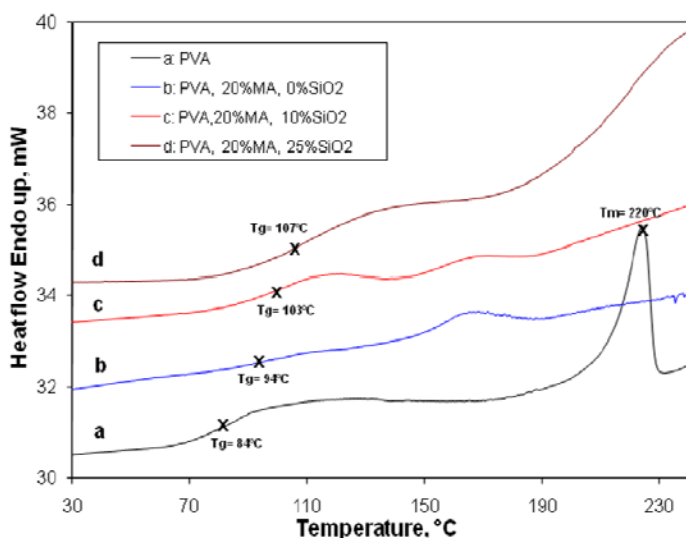

Figure 7. DSC curves of PVA and its hybrid membranes.

3.4 Swelling studies and contact angle

The swelling of any polymer film in a solvent depends upon the diffusion coefficient of the solvent, the relaxation rate of the amorphous regions of the polymer chain and its degree of crystallinity [19]. Table 1 shows the swelling properties of pure PVA and hybrid membranes.

Table 1: Swelling properties of PVA and its hybrid membranes.

Sample details	Swelling degree, %
PVA	301±25%
PVA, 20%MA	61±5%
PVA, 20%MA, 10%SiO$_2$	22±2%
PVA, 20%MA, 25%SiO$_2$	11±1%

The PVA used in the study has a degree of hydrolysis >98% and possesses a large number of hydroxyl group with extensive hydrogen bonding. Pure PVA membrane showed a very high degree of swelling in cold water. This is due to the relaxation of the amorphous region. For the PVA/MA membrane, the swelling was greatly suppressed. This could be explained by the grafting or crosslinking of the PVA polymer chains via an ester linkage between PVA and MA. Esterification of PVA with MA involves the reaction between carboxylic groups of MA and the hydroxyl group of PVA chains, resulting in intermolecular and intramolecular type ester linkages (see Figure 8).
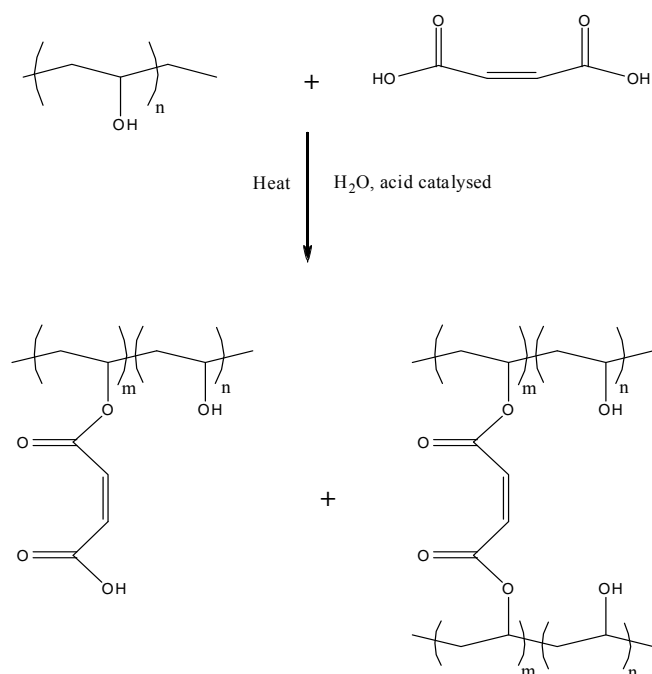

Figure 8. Reaction scheme of PVA with MA.

For PVA/MA/silica membranes, the swelling was further suppressed with the addition of silica. This could be explained by the formation of chemical bonds between polymer and silica. Figure 9 shows reaction schemes of PVA and MA with TEOS. The silica, generated from the hydrolysis and condensation of TEOS, linked with the organic polymer chains through the polar hydroxyl group of PVA and carboxylic group of MA in the polymer. This results in a dense inorganic network and rigid hybrid structure. Therefore, the extent of the water absorption for hybrid membrane was greatly suppressed. Similar findings were also reported by Kotoky and Dolui [22]. There was a considerable decrease in the water absorption in the PVA/silica hybrid films and the swelling in water was greater for those samples with less incorporated silica.
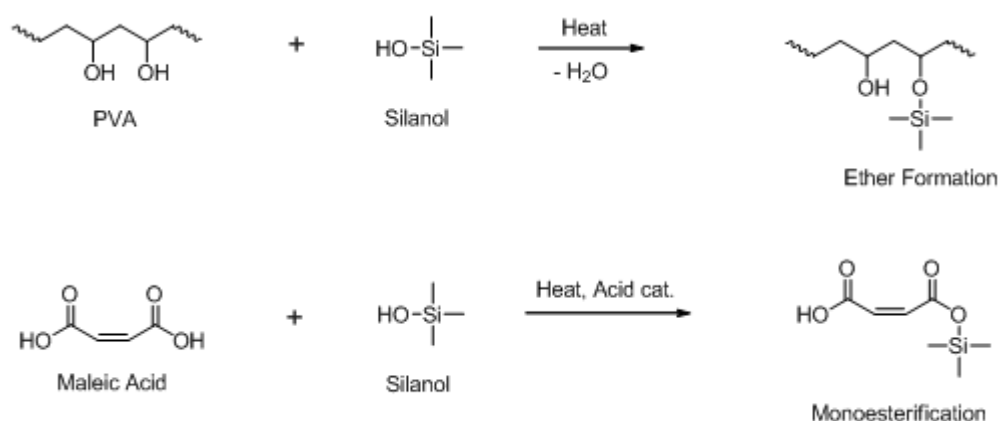

Figure 9. Reaction scheme of PVA and MA with TEOS.

Table 2 shows the water contact angles of PVA and its hybrid membranes. Overall, all membrane samples were hydrophilic. Pure PVA film was very hydrophilic, with a water contact angle of 45.3°. With the incorporation of MA and silica, the contact angle increased, indicating that the surface of the hybrid membrane became more hydrophobic. When MA and silica were incorporated with PVA, the crosslinking among PVA, MA and TEOS led to the consumption of –OH group. Therefore, the hydrophobicity increased.

Table 2: Water contact angle of PVA and its hybrid membranes.

Sample details	Contact angle, ±2 degree
PVA	45.3
PVA, 20%MA, 0% SiO_2	59.4
PVA, 20%MA, 10%SiO_2	63.5
PVA, 20%MA, 25%SiO_2	79.4

3.5 Pervaporation testing

Figure 10 shows the pervaporation desalination performance of PVA/MA/silica hybrid membranes with same thickness (5 μm) at a feed temperature of 22°C and a vacuum of 6 Torr. All prepared membranes had the same amount of MA (20 wt% with respect to PVA) but various silica contents (0-25 wt% with respect to PVA). Overall, the PVA based hybrid membranes demonstrated good desalination performance with high flux (>3.65 kg/m^2·hr) while maintaining a high salt rejection (>95.5%). The salt rejection increased with the silica content and achieved >99.5%. The water flux increased at first but then decreased with increasing silica content. The PVA/MA/silica membrane containing 20 wt% MA and 10 wt% silica gave a high flux of 5.51 kg/m^2·hr.
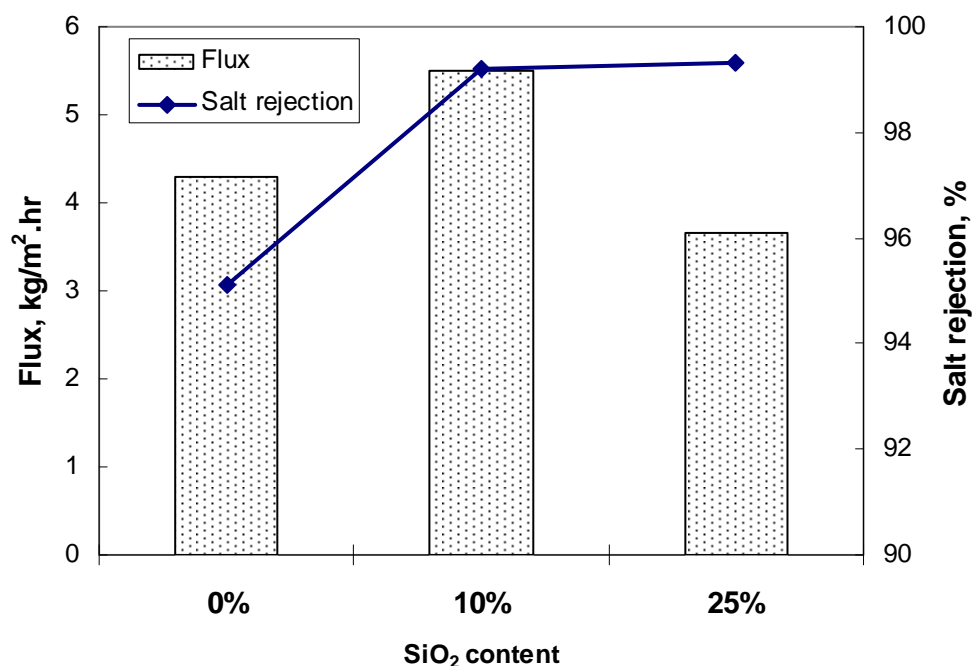

Figure 10. Pervaporation testing results of hybrid membranes (all containing 20 wt% MA with respect to PVA, feed flowrate 30 mL/min, feed temperature 22°C, vacuum 6 Torr).

The solution-diffusion model is usually used to describe the transport mechanism of the pervaporation process which involves three steps: sorption at the membrane surface, diffusion through the dense membrane and desorption into the vacuum [23]. Under the high vacuum used in the study, the desorption step on the permeate side of the membrane is believed to be a fast step and diffusion is generally considered to be the controlling step [2]. In the solution step, the sorption selectivity is more dependent on the affinity between the PVA and the permeants [15]. As mentioned earlier, all the hybrid membranes prepared in the study were hydrophilic (Table 2). This hydrophilic property provides a strong driving force for water affinity and its sorption. As a result, water is both preferentially dissolved and transported in the hydrophilic membranes due to its much smaller molecular size and ability to hydrogen bond. In addition, NaCl is a non-volatile compound. Therefore, the salt rejection remained high for all the membranes as water could be selectively diffused and permeated into the membrane. For PVA/MA membrane with 0% silica, it showed a higher degree of swelling compared to the PVA/MA/Silica membranes (Table 1). Therefore, a small fraction of hydrated salt molecules could possibly diffuse through the membrane under swelling conditions, which led to only 95.5% salt rejection. With increasing silica content, the degree of crosslinking increased and the membrane structure became more compact. Consequently,

the salt rejection increased to nearly 100%.

As the silica content increased, salt rejection increased due to an increase of the degree of crosslinking. It was expected the water flux would consequently decrease due to lower sorption selectivity for water resulting from the increased hydrophobicity (Table 2) upon depletion of hydrophilic hydroxyl groups. However, it was noted that both flux and salt rejection increased for PVA/MA/silica membrane containing 10% SiO_2. This may be attributed to size effect of silica nanoparticles dispersed in the polymer matrix. The incorporation of silica particles in the polymer chain at the nano-scale may disrupt the polymer chain packing and increase free volume, therefore leading to an increase in both water flux and salt rejection. Previous study by Peng *et al.* has demonstrated that introducing inorganic silica derived from γ-(glycidyloxypropyl)trimethoxysilane (GPTMS) into PVA increased free volume and simultaneously enhanced both permeation flux and separation factor in pervaporation of benzene/cyclohexane mixtures [24]. In their study, they also reported that the remarkable increase in free volume cavity was only observed at the lower GPTMS content. Further increase of GPTMS content had no enhancing effect on free volume and small free volume cavity radius even decreased when the weight ratio of GPTMS/PVA was increased from 0.2 to 1.2. As a consequence, the permeate flux increased first and then decreased with increasing GPTMS content [24]. This is consistent with our current finding. The water flux increased first when silica content was increased from 0 to 10 wt% but then decreased when the silica content was increased further to 25 wt%. This could be due to further increase of the silica content from 10 to 25 wt% having negative impact on free volume. In addition, the increased hydrophobicity (Table 2) of membrane would result in less accommodation for water during the diffusion process. Therefore, the water flux decreased.

Another set of experiments was carried out to study the effect of the membrane thickness on the pervaporation desalination performance of aqueous salt solution. A series of hybrid PVA/MA/silica membranes with varying thickness (6-110 μm) were prepared and results are shown in Figure 11. As the membrane thickness increased from 6 to 110 μm, the salt rejection remained constantly high (>99%) and the water flux gradually decreased from 6.93 to 0.82 kg/m^2·hr. With increasing membrane thickness, the resistance across membrane increases, therefore the water flux decreases. According to the solution-diffusion model, at steady state, diffusion flow is constant and there is an inverse relationship between the flux and membrane thickness [13, 23, 25]. Figure 12 shows a linear relationship between the water flux and the reciprocal of the membrane thickness, as predicted by the Fick's law from the solution-diffusion model (Eqution 5). Işıklan and Şanlı also reported that the permeation rate was proportional to the reciprocal of membrane thickness on the pervaporation performance of acetic acid-water mixtures through malic acid modified PVA membranes [13]. Therefore, for this system diffusion through the membrane is rate limiting.
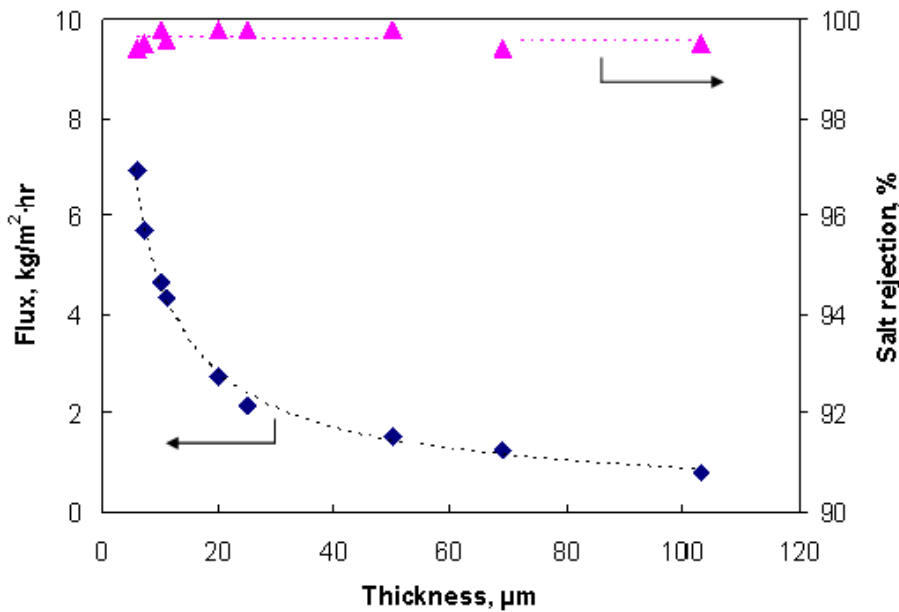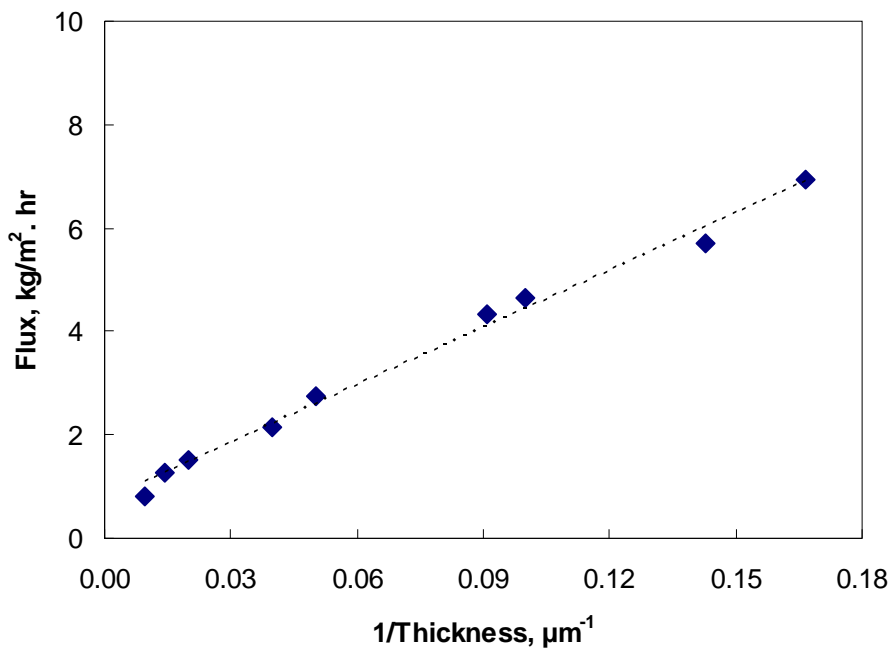
Figure 12. Water flux versus the reciprocal of the membrane thickness.

The apparent diffusion coefficients of water through various PVA based hybrid membranes are displayed in Table 3. It was noted that the diffusion coefficients of water increased first with the addition of silica and then decreased with the further increase of silica content. The PVA/MA/silica membrane containing 20 wt% MA and 10 wt% silica had a highest diffusion coefficient of 7.67 x10^{-12} m^2/s. It is known the diffusivity is generally dependent on both the size of the penetrant and the polymer structure [17]. As water has a very small molecular size (0.278 nm), the diffusion of water through membrane is more determined by the nanostructure of the membrane. PVA is a semicrystalline polymer. The crystalline region is impermeable to the water. This reduces the chain mobility and increases the path length of diffusion. When MA and silica is introduced into the polymer chain, the amorphous region of the membrane increases (as confirmed by the WAXD

14

results in Fig. 5). This favours the diffusion of water molecules, results in the increase in diffusion coefficient when silica content was increased from 0 to 10%. With further increasing silica content from 10 to 25%, the polymer chains became less mobile due to the increased crosslinking density and reduced swelling (Table 1). These combined effects lead to a decrease in the diffusion coefficient.

Table 3: Apparent diffusion coefficient of water for PVA based hybrid membranes.

Sample details	Diffusion coefficient (10^{-12} m^2/s)
PVA, 20%MA, 0% SiO$_2$	5.97
PVA, 20%MA, 10%SiO$_2$	7.67
PVA, 20%MA, 25%SiO$_2$	5.08

4. CONCLUSIONS

A new type of PVA/MA/silica hybrid membranes has been synthesised via a sol-gel route and a solution casting method. Tetraethoxy-silane (TEOS) was used as the silica precursor for sol-gel reaction and MA was added as an additional crosslinking agent. The prepared membrane samples were annealed at 140°C for 2 hr to complete the polycondensation reaction of TEOS and the esterification between PVA and MA. FTIR results confirmed the crosslinking among PVA, MA and TEOS which decreased the crystallinity of hybrid membranes. As a result, this led to a more compact structure with increase amorphous region. SEM images indicated that silica nanoparticles were uniformly dispersed at less than 10 nm scales in the polymer matrix. The thermal properties of the hybrid membranes were significantly enhanced when compared with pure PVA membrane. Water uptake measurement of membranes confirmed that the swelling of hybrid membranes in water was greatly suppressed. Pervaporation testing results on separating aqueous NaCl solution demonstrated a potential application of this type of hybrid membrane for desalination. A high flux of 6.93 kg/m^2·hr and salt rejection above 99.5% could be achieved at a 6 Torr vacuum and 22°C. The hydrophilic nature of hybrid membranes provides a strong driving force for water affinity and its sorption, consequently water is preferentially dissolved and transported through the membranes. Incorporation of silica nanoparticles into the polymer matrix may enhance the free volume of the membrane and diffusion of water molecule through the membrane, and thus enhanced both water flux and salt rejection. However, there is an optimum silica content for achieving the best pervaporation performance. The PVA/MA/silica membrane containing 20 wt% MA and 10 wt% silica had the highest water diffusion coefficient of 7.67 x10^{-12} m^2/s and the highest salt rejection. The effect of membrane thickness on water flux followed the solution-diffusion model, with the flux decreased with the increasing thickness. The salt rejection remained high with varying membrane thickness due to its non-volatile nature.

REFERENCES

[1] Y. P. Kuznetsov, E. V. Kruchinina, Y. G. Baklagina, A. K. Khripunov and O. A. Tulupova, *Russian Journal of Applied Chemistry* **80** (2007), pp 790.

[2] S. S. Kulkarni, A. A. Kittur, M. I. Aralaguppi and M. Y. Kariduraganavar, *Journal of Applied Polymer Science* **94** (2004), pp 1304.

[3] H. J. Zwijnenberg, G. H. Koops and M. Wessling, *Journal of Membrane Science* **250** (2005), pp 235.

[4] B. Bolto, M. Hoang and Z. Xie, *Water AWA* **37** (2010), pp 77.

[5] Z. Xie, D. Ng, M. Hoang, T. Duong and S. Gray, *Desalination* (2010).

[6] R. Tamaki and Y. Chujo, *Applied Organometallic Chemistry* **12** (1998), pp 755.

[7] M. Ulbricht, *Polymer* **47** (2006), pp 2217.

[8] R. Guo, X. Ma, C. Hu and Z. Jiang, *Polymer* **48** (2007).

[9] F. Peng, L. Lu, H. Sun and Z. Jiang, *Journal of Membrane Science* **281** (2006), pp 600.

[10] B. Bolto, T. Tran, M. Hoang and Z. Xie, *Progress in Polymer Science* **34** (2009), pp 969.

[11] T. Q. Nguyen, A. Essamri, S. Pierre and J. Neel, *Makromol. Chem.* **194** (1993), pp 1157.

[12] C.-K. Yeom and K.-H. Lee, *Journal of Membrane Science* **109** (1996), pp 257.

[13] N. Isklan and O. Sanl, *Chemical Engineering & Processing* **44** (2005), pp 1019.

[14] L. Y. Ye, Q. L. Liu, Q. G. Zhang, A. M. Zhu and G. B. Zhou, *Journal of Applied Polymer Science* **105** (2007), pp 3640.

[15] T. Uragami, K. Okazaki, H. Matsugi and T. Miyata, *Macromolecules* **35** (2002), pp 9156.

[16] Q. G. Zhang, Q. L. Liu, Z. Y. Jiang and Y. Chen, *Journal of Membrane Science* **287** (2007), pp 237.

[17] J. P. G. Villaluenga, P. Godino, M. Khayet, B. Seoane and J. I. Mengual, *Industrial & Engineering Chemistry Research* **43** (2004), pp 2548.

[18] E. F. d. Reis *et al.*, *Materials Research* **9** (2006), pp 185.

[19] J. M. Gohil, A. Bhattacharya and P. Ray, *Journal of Polymer Research* **13** (2006), pp 161.

[20] F. Orgaz-Orgaz, *Journal of Non-Crystalline Solids* **100** (1988), pp 115.

[21] M. C. Burshe, S. B. Sawant, J. B. Joshi and V. G. Pangarkar, *Separation and Purification Technology* **12** (1997), pp 145.

[22] T. Kotoky and S. K. Dolui, *Journal of Sol-Gel Science and Technology* **29** (2004), pp 107.

[23] A. Heintz and W. Stephan, *Journal of Membrane Science* **89** (1994), pp 143.

[24] F. Peng *et al.*, *Journal of Membrane Science* **275** (2006), pp 97.

[25] S. C. George and S. Thomas, *Prog. Polym. Sci.* **26** (2001), pp 985.